muscle fibers and fast skeletal muscle fibers, then the differences observed in various aspects of this tension recovery may reflect important differences in the cross-bridge mechanism in the two muscle types. To determine whether similar processes underlie the fast phase for the two muscle types, stiffness in the single SMC was assessed with sinusoidal (250 Hz) length perturbations of small amplitude during the fast phase of tension recovery. In single SMC, as in fast skeletal muscle fibers (*12*), stiffness changed less during the fast phase of tension recovery than might be expected from the known relationship of steady-state force and stiffness. This suggests that similar processes may underlie the fast phases of tension recovery in smooth muscle and fast skeletal muscle. In fast skeletal muscle, this phase of tension recovery has been interpreted as reflecting transitions of a portion of the attached cross-bridge population from an attached low-force state to a high-force state. Therefore, this transition may be much slower in smooth muscle as predicted by our data.

During the fast phase, the rate of recovery varied little as the magnitude of release was increased, but increased as the magnitude of the stretch was increased (Fig. 1F). This length dependence of the rate constant for rapid tension recovery in single SMC is opposite to that observed in fast skeletal muscle fibers; in the latter, the rate constant increases in magnitude from the largest stretches to the largest releases (*6*). Tension transients in slow skeletal muscle fibers of the tortoise (*13*) show a length dependence of the rate constant during the fast phase of tension recovery similar to that in our SMC. Tortoise skeletal muscle is similar in structure to fast skeletal muscle (*14*) but resembles smooth muscle in the high economy of its contraction (*15*). The similarity in the length dependence of the rate constant in the slow skeletal muscle of the tortoise and in SMC may indicate that differences in the inherent length dependence of steps in the cross-bridge cycle may be a common feature of slow economical muscles.

Our results indicate that information about the cross-bridge mechanism can be obtained directly at the cellular level. The tension transients observed in a single SMC suggest that the elasticity of cross-bridges in smooth muscle is linear and more compliant than the elasticity of cross-bridges in fast skeletal muscle and that transitions between attached cross-bridge states occur at least an order of magnitude more slowly in smooth muscle. Further analysis of the tension transient in single smooth muscle cells should aid our understanding of the characteristic ability of smooth muscle to produce forces equivalent to those of striated muscle while using much less energy and having considerably less myosin.

DAVID M. WARSHAW
FREDRIC S. FAY
Department of Physiology, University of Massachusetts Medical School, Worcester 01605

References and Notes

1. F. S. Fay, D. D. Rees, D. M. Warshaw, in *Membrane Structure and Function*, E. E. Bittar, Ed. (Wiley, New York, 1981), vol. 4, p. 79; R. A. Murphy, *Blood Vessels* **13**, 1 (1976).
2. A. F. Huxley and R. M. Simmons, *Nature (London)* **233**, 533 (1971); R. J. Podolsky, A. C. Nolan, S. A. Zaveler, *Proc. Natl. Acad. Sci. U.S.A.* **64**, 504 (1969).
3. W. Halpern, M. J. Mulvany, D. M. Warshaw, *J. Physiol. (London)* **275**, 85 (1978); M. J. Mulvany, *Biophys. J.* **26**, 401 (1979); R. J. Paul and J. W. Peterson, in *Excitation-Contraction Coupling in Smooth Muscle*, R. Casteels, T. Godfraind, J. C. Ruegg, Eds. (Elsevier, Amsterdam, 1977), p. 455.
4. P. Hellstrand and B. Johansson, *Acta Physiol. Scand.* **106**, 221 (1979).
5. F. S. Fay, *I.N.S.E.R.M. Symp.* **50**, 327 (1976); ———, R. Hoffmann, S. Leclair, P. Merriam, *Methods Enzymol.* **85**, 284 (1982).
6. L. E. Ford, A. F. Huxley, R. M. Simmons, *J. Physiol. (London)* **269**, 441 (1977).
7. M. J. Mulvany and D. M. Warshaw, *ibid.* **314**, 321 (1981).
8. F. T. Ashton, A. V. Somlyo, A. P. Somlyo, *J. Mol. Biol.* **98**, 17 (1975).
9. F. S. Fay, K. Fogarty, K. Fujiwara, R. Tuft, in *Basic Biology of Muscles*, B. H. Twarog, R. J. C. Levine, M. M. Dewey, Eds. (Raven, New York, 1982), p. 143.
10. F. S. Fay and J. J. Singer, *Am. J. Physiol.* **232**, C144 (1977).
11. S. B. Marston and E. W. Taylor, *J. Mol. Biol.* **139**, 573 (1980); R. J. Paul, E. Gluck, J. C. Ruegg, *Pfluegers Arch.* **361**, 297 (1976); M. J. Siegman, T. M. Butler, S. V. Mooers, R. E. Davies, *J. Gen. Physiol.* **76**, 609 (1980).
12. F. J. Julian and D. L. Morgan, *J. Physiol. (London)* **319**, 193 (1981).
13. P. Heinl, H. J. Kuhn, J. C. Ruegg, *ibid.* **237**, 243 (1974).
14. S. G. Page, *ibid.* **197**, 709 (1968).
15. R. C. Woledge, *ibid.*, p. 685.
16. This work was supported by the Muscular Dystrophy Association and by grants HL 05770 (to D.M.W.) and HL 14523 (to F.S.F.) from the National Institutes of Health. We thank M. Kawai, R. Moss, L. Mulieri, and S. Taylor for constructive criticism.

21 June 1982; revised 30 August 1982

Overproduction and Elimination of Retinal Axons in the Fetal Rhesus Monkey

Abstract. *Quantitative electron microscopic analysis reveals 2.85 million retinal axons in fetal rhesus monkeys—a number that is more than twice the 1.2 million present in the adult. More than 1 million supernumerary optic axons are eliminated before birth, simultaneously with the segregation of inputs from the two eyes into separate layers of the lateral geniculate nucleus. Selective elimination of optic axons may not only play a role in the segregation of binocular visual connections but, secondarily, may establish the ratio of crossed and uncrossed retinogeniculate projections.*

In all vertebrate species the eyes are connected with the brain by the optic nerve, which contains axons that originate from retinal ganglion cells and terminate in several diencephalic and mesencephalic structures. As a rule, the two optic nerves converge and cross the midline in the form of an X-shaped optic chiasm before reaching the brain. In most mammals a certain number of fibers do not cross the midline but project instead to the ipsilateral side of the brain. The proportion of crossed to uncrossed fibers generally correlates with the degree of overlap between the two visual fields (*1*). Thus, in rodents with laterally

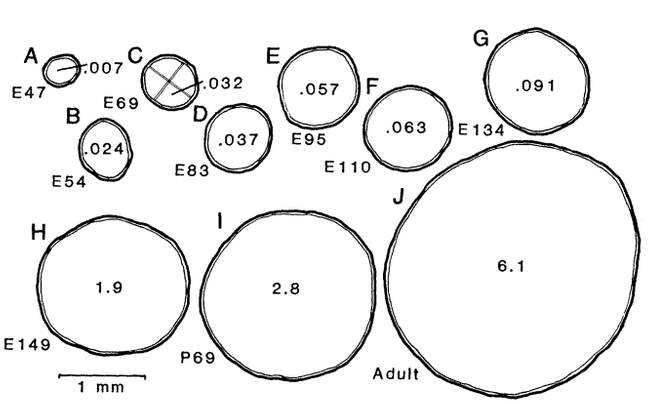

Fig. 1. Cross-sectional areas of 11 optic nerves in a series of monkeys of ascending ages. The thin line marks the nerve boundary, and the thick one, the meningeal membrane. The two diagonal stripes on nerve C illustrate orientations of the electron microscopic photomontages used for quantitative analysis (for example, Fig. 2A).

placed eyes and a minimal visual field overlap, only a small percentage of retinal fibers are uncrossed, whereas in species with eyes closer to the midline and a larger overlap of visual fields, the proportion of uncrossed fibers is larger (*2*). In most primates the eyes are placed forward and their visual fields exhibit virtually total overlap. In such species almost half of the fibers are uncrossed (*1*, *2*) and, in general, the numbers of crossed and uncrossed fibers are roughly proportional to the size of the territories occupied by their terminals in the dorsal lateral geniculate nucleus (LGd). In rhesus monkeys and humans with a six-layered LGd, layers 1, 4, and 6 receive input from the opposite eye and layers 2, 3, and 5 from the eye of the same side (*3*).

The mechanism by which optic axons become distributed to the two sides of the brain and terminate in separate layers of the LGd has been a major conceptual issue in developmental neurobiology (*4*). Of particular relevance to this issue is the recent discovery that projections from the two eyes are first intermixed in the LGd and only later become segregated into appropriate laminar territories (*5*). This finding could be explained either by rearrangement of terminal branches or by selective elimination of inappropriate connections. According to the selective elimination hypothesis supernumerary axons from one eye would retreat from layers 2, 3, and 5 in the ipsilateral and 1, 4, and 6 in the contralateral LGd. Two basic conditions are necessary (but not sufficient) for validating the selective elimination hypothesis: (i) at some point in development the monkey must have at least twice as many optic axons as the adult and (ii) the time course of elimination of most optic fibers must coincide with the period of segregation of projections from the left and right eye within the LGd. We have tested these two conditions in the study reported here.

Eleven rhesus monkeys (*Macaca mulatta*) ranging in age from the 47th embryonic day (E47) to adulthood were fixed by vascular perfusion with 1 percent

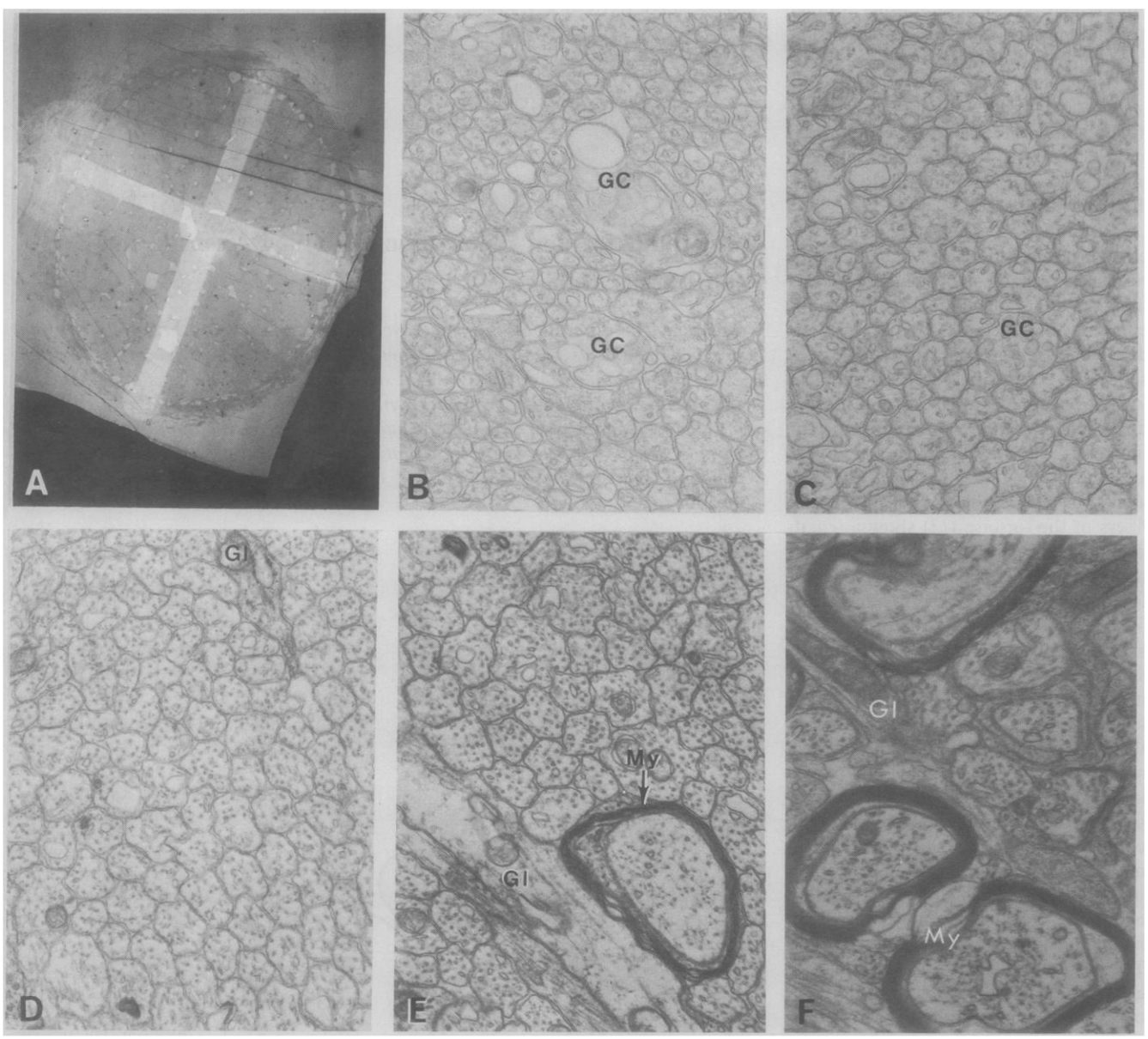

Fig. 2. (A) Low power (×90) electron micrograph of the transected optic nerve from an E69 monkey fetus, showing the two diagonal stripes bleached by the electron beam. The stripes are wider than the actual width of the photomontages (Fig. 1C). (B–F) Higher power (×20,000) electron micrographs of the optic nerves at selected embryonic ages: (B) E47, (C) E69, (D) E83, (E) E110, and (F) E149. Note the presence of axonal growth cones (*GC*) at earlier ages and the development of myelin sheaths (*My*) by E110. Abbreviation: *Gl*, glia.

glutaraldehyde and 1.25 percent paraformaldehyde in phosphate buffer. The optic nerve was dissected midway between the eyeball and the optic chiasm and embedded in Epon-Araldite. Thick (1 μm) sections were stained with toluidine blue and drawn to determine cross-sectional areas (Fig. 1). Adjacent thin (50 nm) sections were placed on Formvar-coated slot grids and stained with lead citrate and uranyl acetate. Electron microscopic montages consisting of overlapping electron micrographs were made across two diagonal radii of the optic nerve (Figs. 1C and 2A) and reconstructed at a final magnification of ×20,000. All profiles of axons, growth cones, glial cells, and other non-neuronal elements were counted, and their cross-sectional areas were measured in each montage. The total number of axons was estimated from the area of the optic nerve and axonal density per unit area.

In agreement with previous studies (*6*) we found that the adult optic nerve in the rhesus monkey contained between 1.2 and 1.3 × 10^6 axons. Slightly different numbers reported by some investigators (*7*) are probably due to methodological rather than to large individual variability. We were able to make reliable comparisons of axonal numbers between animals of different ages because the methods of tissue preparation and counting of axons were the same in all specimens.

During development, the cross-sectional area of the optic nerve steadily increased (Fig. 1), whereas the number of axons showed a rapid initial increase followed by a biphasic decrease. In the E47 embryo retinal axons were unmyelinated and uniform in diameter (Fig. 2B), and they numbered 0.74 × 10^6. Within 1 week, the number of axons almost tripled and surpassed that found in the adult (Fig. 3). Thus, in the E54 specimen the optic fiber count reached 2.0 × 10^6. A still higher complement of axons, 2.85 × 10^6, was found in a fetus killed at E69. This value exceeded the adult number by a factor of 2.2 as did axon counts in fetuses killed over the next 3 weeks (Fig. 3). Although our [^{3}H]-thymidine autoradiographic analysis indicates that all retinal ganglion cells were generated before E80 (*8*) (arrow B in Fig. 3), axonal growth cones in the optic nerve were present until E95. Given that the peak axon count did not change over a 3-week period, it is probable that the actual number of generated axons was even higher than the maximum values reported here.

After E95 the number of axons began to decrease rapidly. By E110, their diameter had become highly variable, with the largest axons beginning to acquire myelin sheaths (Fig. 2E). In the E110 fetus the number of optic axons was 1.9 × 10^6 and in E135 and E149 specimens the number had further diminished to 1.7 and 1.8 × 10^6, respectively (Fig. 3). Although few degenerating axonal profiles were detectable, their number does not reflect the magnitude of fiber loss during this stage, probably because of the rapid removal of cellular debris in embryonic tissue. In spite of the reduction in axon number, the cross-sectional area of the nerve continued to increase because of the enlargement of fibers and the expansion of non-neuronal elements including myelin, which envelops about one-third of optic axons in term fetuses (Figs. 1 and 2F). After birth, the number of axons decreased at a much slower rate (Fig. 3), reaching a value of about 1.6 × 10^6 by the end of the second postnatal month. By this time all optic fibers were myelinated.

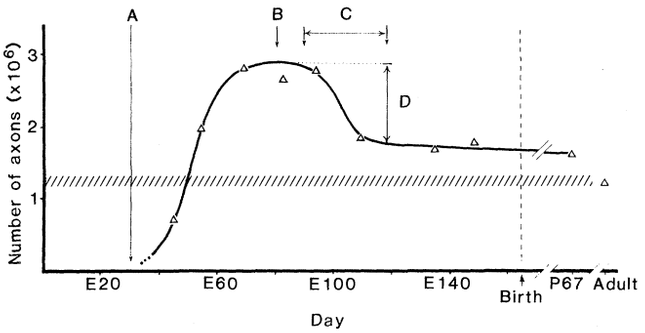

Fig. 3. Number of axons in the optic nerve in rhesus monkeys of various embryonic (*E*) and postnatal (*P*) ages. The striped line indicates the number of optic axons in adult monkeys. Arrow A points to the fetal age, according to our [^{3}H]thymidine autoradiographic analysis (*8*), of the genesis of retinal ganglion cells; arrow B indicates when it stops. C denotes the period when retinal input from the two eyes becomes segregated in the LGd (*5*), which coincides with the period when more than 1 million optic axons are eliminated (vector D).

Our results provide evidence that both conditions essential for the selective elimination hypothesis are fulfilled in the developing monkey. (i) The number of optic tract axons at embryonic periods was more than twice the number present in the adult. (ii) The dramatic reduction in axonal number occurred synchronously with the segregation of retinal terminals from the two eyes into separate territories of the LGd (*5*). Thus, 1 million axons were eliminated during the segregation phase, which occurs between E90 and about E120 (D in Fig. 3). The number of eliminated fibers resembles the number of optic axons present in the adult and theoretically allows clearing of the three out of six cellular layers in each LGd. The period of rapid decrease in retinal input also coincides with the emergence of six layers (*8*) and with a burst of synaptogenesis in LGd (*9*). Since monocular enucleation at or before E90 prevents terminal segregation of retinal input as well as cellular lamination in the LGd (*10*), one can expect that lack of competition between the inputs from the two eyes may arrest the normal elimination of axons (*11*) and secondarily affect cellular events in the LGd (*10*). Our findings, of course, do not exclude the possibility that some terminals are relocated, as occurs in the cortex during segregation of ocular dominance columns (*12*).

The selective elimination hypothesis is attractive because it invokes interaction between peripheral and central structures to explain both the segregation of retinal terminals in the LGd as well as the ratio between crossed and uncrossed fibers at the chiasm. A previous study has indicated that prior to E90 each eye projects equally to both ipsilateral and contralateral LGd's (*5*). Therefore, elimination of retinal input from three of the six layers in each LGd could result in an approximately 1:1 ratio of crossed to uncrossed fibers. Since the number of optic axons in adult monkeys and humans are similar (*13*) and since both species have similar ratios of crossed to uncrossed fibers (*3*) and similar distributions of terminals in the LGd (*1, 3*), our data also provide insight into normal and pathological development of the human visual system.

If selective elimination of axons play a role in establishing the ratio of crossed to uncrossed fibers, one could predict that in mammals with a smaller portion of the LGd innervated by the ipsilateral eye, a smaller fraction of crossed fibers would be eliminated. Obviously, any prediction about the extent of such elimination must take into account both the initial and final ratio of crossed and uncrossed fibers, which may be different in each species. For example, birds which have completely crossed optic tracts as adults nevertheless contain supernumerary optic axons as embryos (*14*), axons that include transient ipsilateral projections (*15*). However, since the retina also projects to structures where axonal elimination may play different roles (*16*), one

could expect a supplemental reduction of axons. Indeed, we found that an additional half million optic fibers or roughly 50 percent of the adult number are deleted during a second, slow phase of elimination that extends into postnatal life (Fig. 3). This late phase of axonal reduction may serve functions unrelated to the establishment of connections mediating binocular vision since cell death, withdrawal of axons, or both seem to be a ubiquitous feature of the developing brain (*17*).

PASKO RAKIC
KATHARINE P. RILEY
Yale University School of Medicine, New Haven, Connecticut 06510

References and Notes

1. G. Wells, *The Vertebrate Eye and Its Adaptive Radiations* (Cranbrook, Bloomingfield Hills, Mich., 1942); S. Polyak, *The Vertebrate Visual System* (Univ. of Chicago Press, Chicago, 1957); J. D. Pettigrew, *Sci. Am.* **227**, 84 (August 1972); J. H. Kaas, R. W. Guillery, J. M. Allman, *Brain Behav. Evol.* **6**, 253 (1972).
2. S. Ramon y Cajal, *Rev. Trimestr. Microgr.* **3**, 15 (1898); W. E. L. Clark, *Physiol. Rev.* **22**, 205 (1942); S. M. Blinkov and J. I. Glezer, *The Human Brain in Figures and Tables* (MIT Press, Cambridge, Mass., 1968).
3. M. Minkowski, *Arch. Neurol. Psychiatry* **6**, 201 (1920); N. R. Matthers, W. M. Cowan, T. P. S. Powell, *J. Anat.* **94**, 145 (1960); A. Hendrickson, M. E. Wilson, M. J. Toyne, *Brain Res.* **23**, 425 (1970); D. H. Hubel, T. N. Wiesel, S. LeVay, *Philos. Trans. R. Soc. London Ser. B* **278**, 377 (1977).
4. R. D. Lund, *Development and Plasticity of the Brain* (Oxford Univ. Press, New York, 1978); R. W. Guillery, *Progr. Brain Res.* **51**, 403 (1979); K. J. Sanderson, *Aust. J. Optom.* **63**, 220 (1980); D. O. Frost, K.-F. So, G. E. Schneider, *Neuroscience* **4**, 1649 (1979).
5. R. Rakic, *Nature (London)* **261**, 467 (1976).
6. S. R. Bruesch and L. B. Arey, *J. Comp. Neurol.* **77**, 631 (1942); T. E. Ogden and R. F. Miller, *Vision Res.* **6**, 485 (1966).
7. A. M. Potts, D. Hodges, C. B. Shelman, D. J. Fritz, N. S. Levy, Y. Mangnall, *Invest. Ophthalmol.* **80**, 980 (1972).
8. P. Rakic, *Philos. Trans. R. Soc. London Ser. B.* **278**, 245 (1977); M. LaVail and P. Rakic, *Invest. Ophthalmol.*, in press.
9. A. Hendrickson and P. Rakic, *Anat. Rec.* **187**, 602 (1977).
10. P. Rakic, *Science* **214**, 928 (1981).
11. G. Jeffery and V. H. Perry, *Dev. Brain Res.* **2**, 176 (1980); D. R. Sengelaub and B. L. Finley, *Science* **213**, 573 (1981); A. Y. K. Ng and J. Stone, *Dev. Brain Res.* **5**, 263 (1982); R. W. Williams, M. J. Bastiani, L. M. Chalupa, *J. Neurosci.* **3**, 133 (1983).
12. S. LeVay and M. P. Stryker, *Soc. Neurosci. Symp.* **4**, 83 (1979).
13. S. R. Bruesch and L. B. Aray, *J. Comp. Neurol.* **77**, 631 (1942); O. Opel, *Arch. Ophthalmol.* **166**, 19 (1963).
14. G. Rager and U. Rager, *Exp. Brain Res.* **33**, 65 (1978).
15. S. C. McLoon and R. D. Lund, *ibid.* **45**, 277 (1982).
16. T. J. Cunningham, *Int. Rev. Cytol.* **74**, 163 (1982); S. C. McLoon, *Science* **215**, 1418, (1982).
17. V. Hamburger, *J. Comp. Neurol.* **160**, 535 (1975); W. M. Cowan and P. G. H. Clarke, *Brain Behav. Evol.* **13**, 345 (1976); L. Landmesser and G. Pilar, *Fed. Proc. Fed. Am. Soc. Exp. Biol.* **37**, 2016 (1978); R. W. Oppenheim, in *Studies in Developmental Neurobiology*, M. W. Cowan, Ed. (Oxford, Univ. Press, New York, 1981), pp. 74–133; G. M. Innocenti, *Science* **212**, 824 (1981).
18. Supported by PHS grant EY02593. Pregnant rhesus monkeys were provided by the breeding colonies at Yale University School of Medicine and the New England Regional Primate Research Center, Southborough, Mass., which is supported by NIH grant RR00168. We wish to thank P. Seghal for surgery and care of the animals. Preliminary versions of these results were presented at a meeting at the NATO Advanced Study Institute, Varenna, Italy, 28 May 1981, and at the 12th Annual Meeting, Society for Neuroscience, Minneapolis, Minn., 31 October to 5 November 1982.

29 July 1982; revised 25 October 1982

A Developmentally Regulated Neuraminidase Activity in *Trypanosoma cruzi*

Abstract. *The human pathogen* Trypanosoma cruzi *(Y strain) contains a neuraminidase activity that varies widely in the different developmental stages of the parasite. The specific neuraminidase activity of infective trypomastigotes obtained from tissue culture and from the bloodstream of infected mice is 7 to 15 times higher than that of the acellular culture forms. Amastigotes were devoid of enzyme activity. The enzyme has a* p*H optimum of 6.0 to 6.5. Live trypanosomes released sialic acid from human erythrocytes and plasma glycoproteins. Several sialyl compounds were hydrolyzed by the parasite, but the best substrate was the protein orosomucoid. Erythrocytes from infected mice with* T. cruzi *parasitemia were agglutinated by peanut lectin and the hemagglutination titer was correlated with the degree of parasitemia.*

Chagas' disease, which results from infection with the protozoan parasite *Trypanosoma cruzi*, is characterized by an acute illness that is followed in some patients by chronic cardiac and gastrointestinal sequelae (*1*). Little is known about the molecular basis of the pathogenic events.

In the experiments described here a developmentally regulated neuraminidase activity was discovered in *T. cruzi* that may be relevant to the pathogenesis of Chagas' disease. Viable parasites released sialic acid from human cells and serum glycoproteins in vitro and from erythrocytes of mice experimentally infected with *T. cruzi*. Erythrocytes that had been incubated with *T. cruzi* were agglutinated by peanut lectin (PNA).

It is widely accepted that sialic acid is involved in physiological processes of mammalian cells and glycoproteins (*2*). Since it is a relatively strong acid (pKa = 2.6), it is essentially completely deprotonated at physiological pH, thereby providing a negative charge at the surface of cells (*3*). Treatment of cells with neuraminidase alters this charge. Plasma glycoproteins and blood cells that have been desialylated are rapidly removed from the circulation and accumulate in the spleen and liver (*4*). Lymphocytes treated with neuraminidase show altered functional properties (*5*). Certain antigens present on the surface of intact cells are more extensively exposed after neuraminidase digestion (*6*). Neuraminidase also has a functional effect on cardiac cells (*7*) and on the neuromuscular junction (*8*). These cells are potentially affected in *T. cruzi*–infected mammals.

The developmental forms of *T. cruzi* were obtained as follows: Epimastigotes were from 5-day-old cultures in an ox liver infusion mixture containing tryptose and supplemented with 10 percent fetal calf serum at pH 7.2 (LIT) (*9*). Trypomastigotes were purified from 20- to 30-day-old LIT cultures on a DEAE-cellulose column (*9*). Bloodstream trypomastigotes were isolated from heparinized blood of 6-day infected CF-1 mice that had been irradiated 2 days before infection with 600 rad from a cesium source (*9*). Trypomastigotes were also obtained from supernatants of primary cultures of newborn human foreskin fibroblasts (*10*). Amastigotes were obtained from the fibroblast cultures 2 to 3 days after the trypomastigotes were harvested. They were washed twice with RPMI-1640 medium and isolated from the 20:25 percent interface of a discontinuous gradient of 15, 20, and 25 percent metrizamide after centrifugation at 1000g for 60 minutes. If the parasites were to be assayed live, they were washed three times in RPMI-1640 medium containing protease inhibitors [2 μM leupeptin, 2 mM phenylmethylsulfonyl fluoride (PMSF)] and 0.02 percent azide as preservative. In the assays with lysed trypanosomes, the organisms ($\sim 10^8$ per milliliter) were centrifuged at 1000g for 10 minutes. The pellet was resuspended to the initial concentration in ice-cold distilled water containing 2 μM leupeptin, 1 mM PMSF, and 0.02 percent sodium azide and washed twice in distilled water at 100,000g for 60 minutes before the enzyme assay (*11*).

The rate of hydrolysis of several sialyl compounds was linear for at least 3 hours in experiments with live parasites or with suspensions of trypanosomes lysed in distilled water under the assay conditions (*11*). The relation between trypanosome concentration (viable and lysed organisms) and enzyme activity